Lau, C. K. & Bolton, M. D. (2011). *Géotechnique* **61**, No. 8, 639–650 [**doi:** 10.1680/geot.7.00207]

The bearing capacity of footings on granular soils. II: Experimental evidence

C. K. LAU* and M. D. BOLTON†

Scale effects, especially stress-level effects, cause considerable confusion in the calculation of bearing capacity on granular soils. A companion paper describes a new method of calculation that explicitly allows for the variation of sec ϕ with mean effective stress p. This approach is validated here for the case of model circular footings on dense beds of silica sand and silica silt. The models were tested at 1g with surcharge to explore the N_q behaviour, and in a centrifuge to determine self-weight effects for N_γ. It is shown that triaxial ϕ values expressed as a function of the logarithm of p can be used to predict model bearing capacities within a deviation in ϕ of 2°.

KEYWORDS: bearing capacity; centrifuge modelling; footings/foundations; model tests; sands; silts

Les effets d'échelle, notamment les effets de niveau de contraintes, donnent lieu à une confusion considérable pour le calcul de la force portante sur des sols granulaires. Une communication faisant penchant à la présente (1ère partie) décrit une nouvelle méthode de calcul, prévoyant de façon explicite la variation de la sécante ϕ avec la tension efficace moyenne p. Cette approche est validée ici pour le cas de maquettes de semelles circulaires sur des lits denses de sable siliceux et limoneux. On a soumis les maquettes à des tests à 1g avec surcharge pour explorer le comportement N_q, et dans une centrifuge, afin de déterminer les effets du propre poids pour N_γ. On démontre que des valeurs triaxiales ϕ, exprimées en fonction du logarithme de p, peuvent être utilisées pour prédire les forces portantes des modèles au sein d'une deviation de 2° sur ϕ.

INTRODUCTION

In their introduction to foundation problems, Terzaghi & Peck (1948) developed the classical bearing capacity equation, and defined bearing capacity factors N_c, N_q, N_γ in terms of a linear strength envelope $\tau_{max} = c + \sigma \tan \phi$. They advised that peak strength parameters should be used for c and ϕ only when the supporting soil would fail in 'general shear' (Fig. 1). They postulated that, otherwise, shear would occur beneath, but not around, the foundation, and proposed that in this case of 'local shear' the peak strength should be reduced by a factor 1·5 to achieve satisfactory designs. This idea was taken up by Vesic (1963). However, subsequent investigators have found difficulty in separating various effects that Terzaghi & Peck were unable to discriminate between. These include: a non-linear peak strength envelope; progressive failure due to strain localisation and softening to critical states; corrections for depth/width ratio by including an allowance for increase of depth (i.e. settlement) during loading; anisotropy; and an allowance for footing shape between a long strip (plane strain) and a circular pad (axisymmetric), which itself must comprise partly a statement regarding appropriate strength parameters (plane strain or triaxial) and partly a recognition that the state of limiting equilibrium is influenced by 3D effects, arching and so on.

De Beer (1965a) reported triaxial tests on sand in which the strength envelope was non-linear, and characterised by a sec ϕ value that increased linearly with the relative density I_D and reduced linearly with the logarithm of mean stress p. For the purposes of this paper, all stresses are effective stresses unless otherwise stated. Bolton (1986) confirmed that these observations were a general feature of the peak strength of sands, and suggested an empirical relation between ϕ, I_D and $\log p$ that took account of the greater strength observed in plane strain compared with axisymmetric (triaxial) strain. De Beer (1965b) developed an understanding of the possible scale effect on footings in terms of a reduction in sec ϕ with p: the bearing capacity factors for large footings carrying high stresses should logically be smaller than those for small footings.

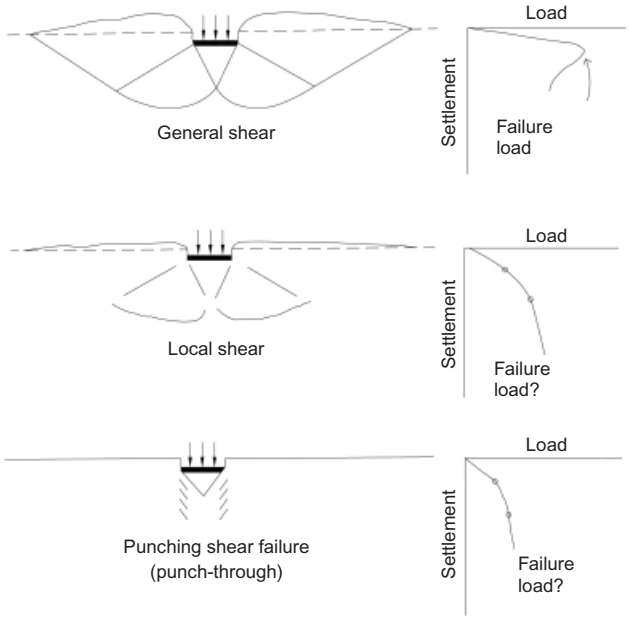

Fig. 1. Modes of failure mechanism (after Vesic, 1963)

The work of De Beer shows that it is essential to re-create correct stress levels in model tests if correct behaviour is to be observed. Ovesen (1975) explained the use of a geotechnical centrifuge to achieve full-size stresses in reduced-scale models of foundations. Ovesen (1979) went on to show that the effect of reducing footing width B while retaining particle size d is negligible, at least when $B/d > 30$.

The non-uniform approach to peak strength, and especially

Manuscript received 27 November 2007; revised manuscript accepted 15 October 2010. Published online ahead of print 25 January 2011. Discussion on this paper closes on 1 January 2012, for further details see p. ii.

* Fong On Geotechnics Limited, Hong Kong.
† Engineering Department, University of Cambridge, UK.

the possibility of progressive failure due to strain concentration in soils with a brittle peak strength, was investigated by Muhs (1965) in footing tests at 1***g***. Yamaguchi *et al.* (1976, 1977) performed centrifuge tests on model footings in which soil strains were measured around the footing, leading to an understanding of the progressive mobilisation of strength in different regions. Non-uniformity of strength, due not to the strain distribution, but to anisotropy leading to reduced ϕ values on slip surfaces parallel to soil bedding, was considered by Tatsuoka *et al.* (1991).

Figure 2 shows, in sketches, the variations of ϕ that might concern a practising engineer who wishes to use some bearing capacity equation to predict the plastic indentation of footings on sand.

In the investigation that follows it has been assumed, following Corte (1989) and Cerato & Lutenegger (2007), that stress level effects in Fig. 2(c) are paramount in the bearing capacity problem. A companion paper (Lau & Bolton, 2011) discusses the use of plasticity theory to predict the bearing capacity of footings where ϕ varies as in Fig. 2(c), and explains how an equivalent constant ϕ might be deduced. Other influences in Fig. 2(b) and Fig. 2(d) will be discussed in the light of the experimental findings.

There is still some interest shown from the oil exploration industry in shallow foundation design principles. This is a result of the use of spudcan foundations for offshore oil rigs (LeBlanc, 1981). Like interpretation of penetrometer data, the main point of interest for spudcan design has always been the evaluation of failure loads. This is because spudcans have to be pushed into the seabed to a predetermined depth with ballast on the rig during preloading before unloading the rig to its normal working conditions. This is partly a safeguard against accidental overloading and scouring of the seabed by under-currents, which may undermine their foundations during their working life. As spudcans can normally reach 20 m in diameter (Randolph *et al.*, 2005), scale effects therefore remain a problem to be resolved.

The methodology adopted for this experimental validation exercise is as follows.

(*a*) It was decided to acquire two granular materials that differed in nominal diameter by a factor of 50, but which were otherwise practically indistinguishable in all other grain characteristics. The idea was that they could be used as model materials for each other.

(*b*) Soil models of different sizes were constructed using the same material for both 1***g*** and centrifuge tests, in order to investigate the relative particle size effects. It has been common practice in Cambridge (Schofield, 1980) to use models of modelling. The idea is to model a centrifuge model with another centrifuge model at a different scale in order to check their internal consistency. The major disadvantage is that the differences in scale between two such centrifuge models are not generally larger than seven.

(*c*) Soil models were constructed of a particular footing bearing on each of the two model soils of different particle size. The footing size : particle size ratio could then be varied over a wide range, while most of the existing laboratory apparatus and equipment could be utilised without much adaptation. This approach inevitably introduced some complications as a result of changing the grain characteristics. In particular, any absolute particle size effects had to be accounted for when interpreting the experimental results.

The soil bed under a 1***g*** condition and with surcharge is designed to derive its resistance to the advancing punch

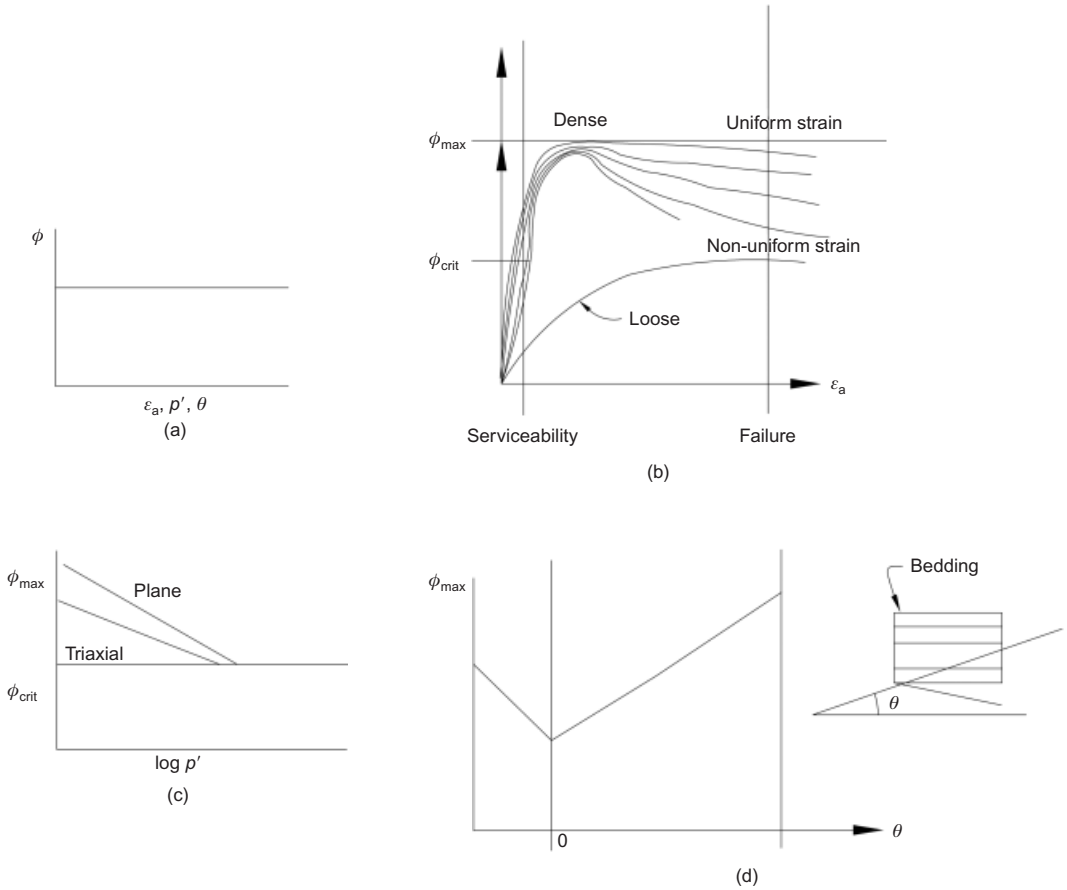

Fig. 2. The variations of ϕ that might concern a practising engineer: (a) ideal soil: bearing capacity equation; (b) $\phi = f(\varepsilon_a)$; (c) $\phi_{max} = f(p')$; (d) $\phi_{max} = f(\theta)$

overwhelmingly from the surcharge term of Terzaghi's equation,

$$\sigma_f = \sigma_o N_q + \tfrac{1}{2} B\gamma' N_\gamma$$

where σ_o is the surcharge, N_q is the bearing capacity factor (surcharge) and N_γ is the bearing capacity factor (self-weight)

To achieve this, the surcharge is applied such that the self-weight at 1$\boldsymbol{g}$ when compared with the surcharge is negligible. Under elevated $\boldsymbol{g}$ conditions in a geotechnical centrifuge, however, the soil can derive its resistance to the advancement of the punch from its self-weight alone. In the event that settlement is significant, correction should be made to account for the effective increase in overburden equivalent to the surcharge, and other geometric effects. By taking advantage of these considerations, it is possible to uncouple the scale effects on N_q and N_γ.

The data are then used to validate the theoretical predictions from the companion paper (Lau & Bolton, 2011), based on plastic solutions by the method of characteristics, and permitting ϕ to vary with p.

MATERIAL ACQUISITION

Two silica soils, a sand and a silt, which differed in nominal grain diameter by a factor of 50 but which were otherwise indistinguishable in terms of shape, grading and mineralogy, were successfully acquired (see Table 1 and Fig. 3). These were

(*a*) silt: washed silica flour
(*b*) sand: 8/40 wires Chatelet flint grit.

SAMPLE/MODEL PREPARATION

On top of stress effects, the bearing capacity is also dependent on I_D. To simplify the validation exercise, the sand and silt beds were placed at their $e \approx e_{min}$. This also facilitated the achievement of uniform density in the models.

Table 1. Properties of the two granular materials

Property	Silt	Sand
Mineralogical make-up	>99% SiO_2	>97% SiO_2
Specific gravity	2·65	2·65
Roundness	0·40	0·41
Sphericity	0·80	0·77
d50: μm	12	600
Permeability: m/s	$3 \times 10-7$	$1{\cdot}7 \times 10-3$
ϕ_{crit}: degrees	37·5	37·5

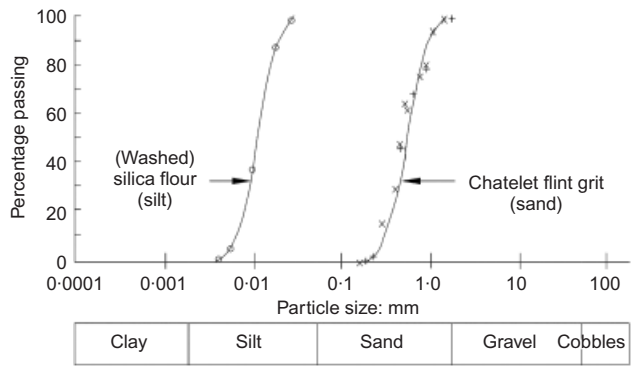

Fig. 3. Grading curves of the two granular materials

The dense sand was laid down by pluviation into the tub at a rate of 1·33 kg/min from a suspended conical hopper by way of a plastic hose 600 mm long, with 28 mm internal diameter, and at a constant drop height of 600 mm. The tub was 850 mm in diameter and 400 mm high. The sand was poured until the target height of the model was slightly passed. A modified vacuum cleaner was used to level the model back down to the target height. The tub was weighed to the nearest 1 kg before and after the sand was placed. When the volume was known, the bulk dry density could be estimated. With this method, e_{min} for the sand was found to be $0{\cdot}60 \pm 0{\cdot}04$.

When a saturated model was required, a steel lid was used to seal the top of the tub and the air inside was evacuated by a vacuum pump. Water was then permitted to percolate upwards through the bottom drain at a flow rate slow enough to ensure that piping would not occur during the saturation process (Lau, 1988).

The saturated silt was compacted by a vibrator bolted onto the wall of the tub. The slurry was introduced into the tub in layers with the vibrator switched on in order to let out any trapped air. When the required amount of slurry was in place and no more air bubbles could be seen escaping through the top of the slurry, which normally took roughly 24 h to achieve, the top of the silt bed was covered with filter paper before a steel piston weighing 345 kg was put on top. Vibration continued until no further settlement of the piston could be observed: this normally took another 48 h. During compaction, both top and bottom drainage was provided. In order to determine the bulk dry density, the tub was weighed to the nearest 1 kg before and after the compacted silt was in place. The volume of the silt was calculated by measuring the thickness of the model with the aid of a template at a regular grid of no less than 96 sampling points. With this method, e for the silt was found to be $0{\cdot}59 \pm 0{\cdot}04$.

Triaxial specimens of the sand were formed similarly by pluviation in a triaxial sample mould. For the silt, eighteen 100 mm cubes were excavated from the previously compacted bed. As soon as they were excavated, the samples were swiftly sealed with cling film with a view to retaining as much moisture as possible until triaxial tests could be carried out later. Immediately before the triaxial test, the sample was put on a lathe and trimmed carefully to the required diameter by a sharp cutting edge, guided by two vertical straight edges. It was then put on a cradle to be trimmed carefully to the required height before mounting in the triaxial cell. The volume was then measured. The dry weight was measured after each test when the specimen was oven-dried.

TRIAXIAL TEST PROGRAMME

It was decided to investigate the absolute particle size and stress effects by triaxial tests conducted over a wide range of effective confining pressures ranging from 10 to 10 000 kPa. In a triaxial test, the stress and strain fields are intended to be uniform; the formation of localised shear in rupture bands is not encouraged, at least before ϕ_{max} has been reached.

The triaxial test results from 38 mm diameter samples tested with smooth platens and a height : diameter ratio of 2 are presented in Figs 4 and 5 as the secant of the angle of friction and volumetric strain against axial strain. The unload–reload loops have been omitted from the plots of ϕ against ε_a plots only for clarity. The secant of the angle of friction is obtained by dropping a tangent from the origin to a single Mohr circle of stress. The attainment of ϕ_{max} in general coincides with the maximum rate of dilation. ϕ_{crit} is not reached in low-pressure tests, as dilation was continuing

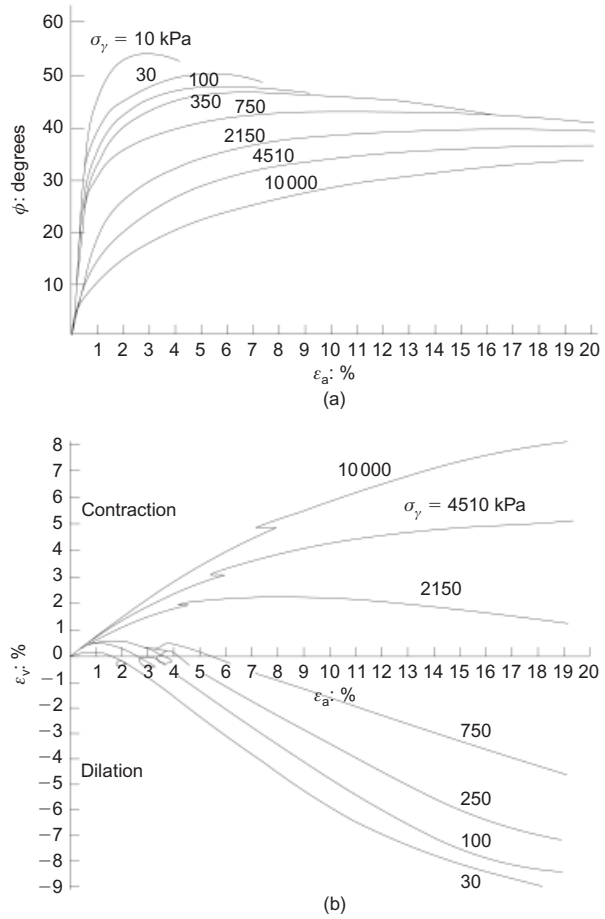

Fig. 4. Effects of effective cell pressure on the stress–strain behaviour of sand in triaxial compression

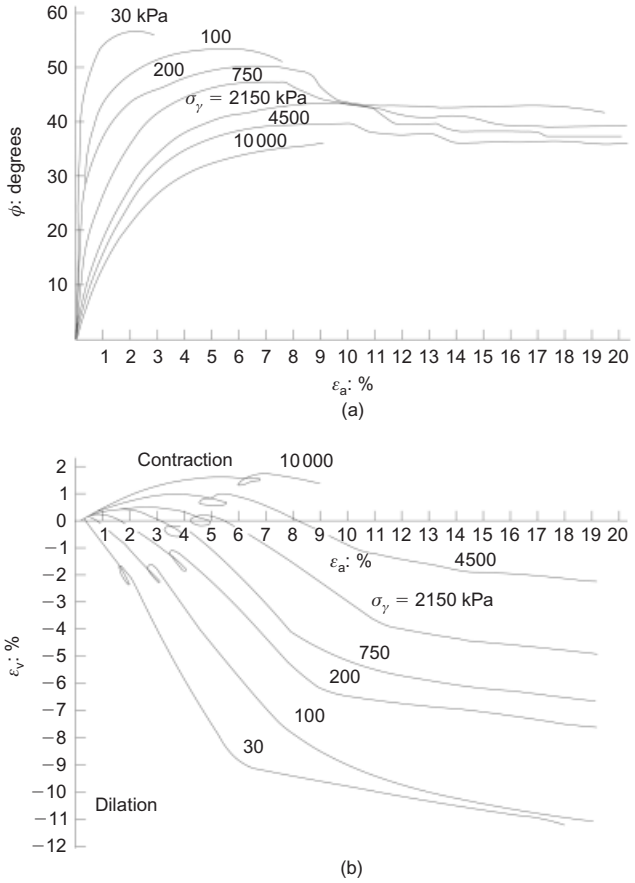

Fig. 5. Effects of effective cell pressure on the stress–strain behaviour of silt in triaxial compression

even after an axial strain of 20%. ϕ_{crit} could be reached, however, when the confining pressure was high enough to suppress all dilation. ϕ_{max} is higher for silt than for sand, and the corresponding rate of dilation is also higher. One interesting observation is that ruptures were obviously formed in the silt samples after ϕ_{max} had been reached, resulting in a sudden decrease in both ϕ and the rate of dilation (see Fig. 5). It is obvious that the interference of ruptures was deferred when cell pressure was higher. Formation of ruptures was not obvious in the sand specimens.

Figure 6 summarises the pressure effects on sec ϕ for the two materials. Sec ϕ is 4–5° higher for the silt than for the sand, but the trend of pressure effects is similar. In both cases, the secant of the angle of friction reduces linearly with the logarithm of mean stress. The results of the sand agree well with Bolton's (1986) empirical correlation for sands, also shown in Fig. 6: the deviation is smaller than ±2°. Shifting of the grading curves shows that crushing occurred during the triaxial tests for sand under high pressure (see Fig. 7). More crushing occurs when the confining pressure is increased. However, no crushing occurs when the sand is subjected to isotropic compression only. It is the crushing of grains that leads to reductions in dilatancy, and thereby to reductions in the angle of shearing resistance.

The silt was able to maintain a higher peak angle of shearing and rate of dilation than the sand in the triaxial tests. At a similar voids ratio (close to minimum) and confining pressure, ϕ_{max} of the silt is 4–5° higher than that of the sand. From Fig. 6 it can equally be said that the silt is about four to five times less stress sensitive than the sand.

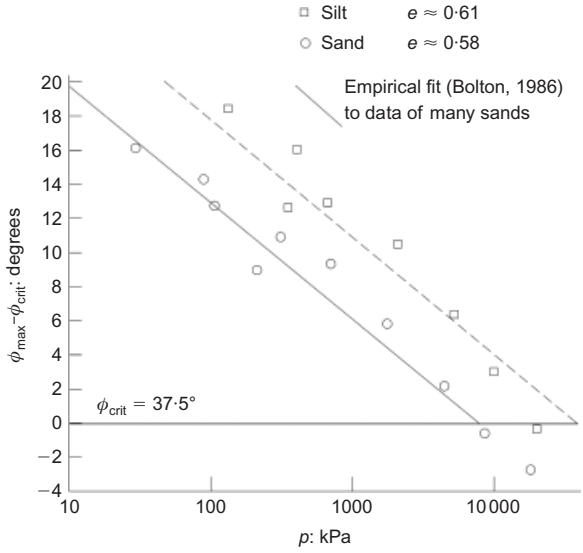

Fig. 6. ϕ_{max} plotted against logarithm of mean stress

This may be explained by the inevitable reduction in the size of flaws in the smaller particles. Griffith's (1921) criterion for fracture proposes that rupture stress is inversely proportional to the square root of the size of a flaw. If the flaws in the silt particles had been scaled down in the same ratio as their diameter (factor 50 compared with the sand), they would have proved about seven times more resistant, rather than five times.

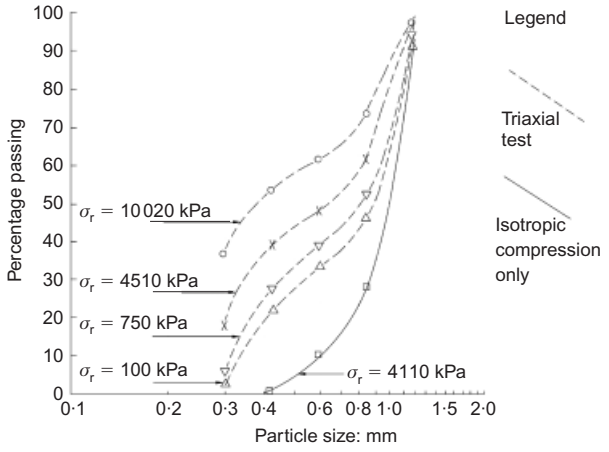

Fig. 7. Grading curves of sand samples after triaxial tests and isotropic compression

1g model tests

The 1***g*** test series was designed to investigate scale effects in footing tests on weightless soil. A schematic layout of the test set-up is shown in Fig. 8. The boundary value problem chosen was a cylindrical bed of soil 850 mm in diameter and 350 mm high. The soil model was either fully submerged in water or dry. The side and bottom of the soil model were assumed to be supported by smooth and rigid boundaries. In order to simulate this smooth condition, the inside of the tub wall was lubricated with plumber's grease. The top surface of the soil model around the punch was subjected to a constant surcharge pressure ranging from 5 to 200 kPa. In this range of surcharge, the soil could practically be treated as weightless. The bottom of the model was a free-draining boundary. To achieve this, a 3·2 mm thick blanket of grade F Vion supplied by Porvair of King's Lynn was used to line the bottom of the tub. The permeability of this drainage blanket is $7{\cdot}5 \times 10^{-5}$ m/s in both the vertical and horizontal directions.

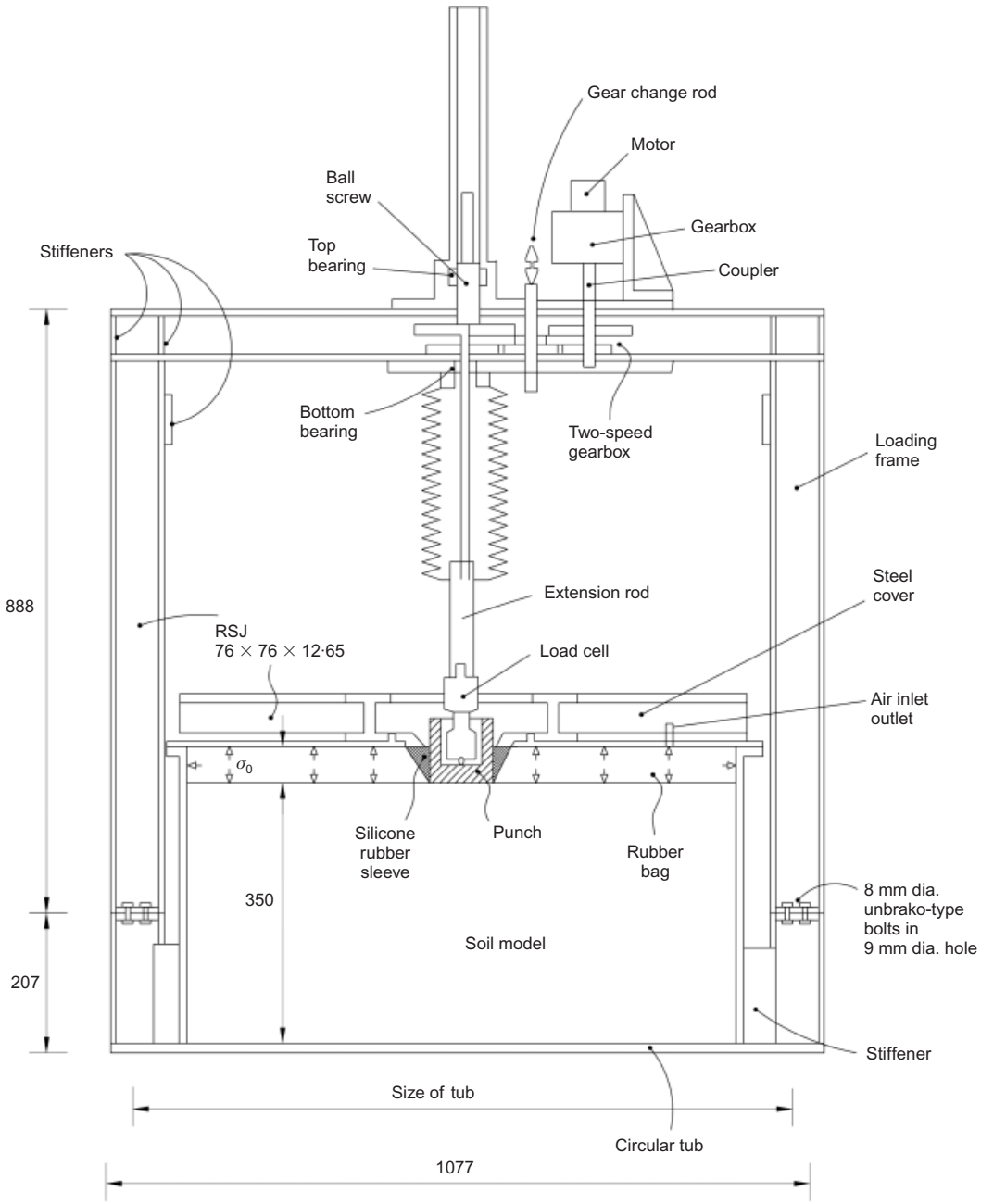

Fig. 8. General layout of test rig at 1*g*

Two punches, one of 100 mm diameter and one of 14·2 mm diameter, were used in the tests. During a test, a centrally placed rough, rigid punch of diameter 100 mm (or 14·2 mm) was pushed axisymmetrically into the soil bed in a displacement-controlled manner in order to facilitate the investigation of post-peak behaviour. Throughout the indentation process, the average bearing pressure under the footing and the settlement of the punch were monitored.

The 1***g*** test programme is summarised in Table 2. The three variables were $B/d_{50,}$ σ_o and $d_{50.}$ Apart from studying the scale effects, this series of tests was also used to investigate the effect of settlement : diameter ratio (w/B) on N_q.

Penetration effects

Figure 9 shows the indentation response in tests 14 (diameter $B = 14$ mm) and 18 ($B = 100$ mm) plotted in terms of footing pressure σ_f against settlement w, and also against non-dimensional settlement ratio w/B, for a surcharge $\sigma_o = 10$ kPa. Two features of Fig. 9 are noteworthy.

(*a*) It must be expected that, in early loading, soil strength should be mobilised as a function of strain, and also that strain must be a function of the only available non-dimensional measure of kinematics, namely w/B. This is well demonstrated in Fig. 9, in which scale effects on settlement prior to plastic indentation are correctly eliminated when settlement ratio w/B is used.

(*b*) Following plastic yielding, there is evidence of a steady enhancement of bearing pressure with settlement ratio for $w/B > 0{\cdot}5$, particularly in test 14. Two possible explanations for this increase might be suggested:
   (i) additional surcharge due to self-weight of the sand overburden now above the current elevation of the footing base
   (ii) additional shear strength being mobilised in the overburden.

However, the overburden effect of 30 mm of sand is only 0·7 kPa, or 7% of σ_o, so the first explanation fails to tally with the observation of a 60% increase in test 14.

The development of strength in the overburden as understood by Meyerhof (1951) demands an extra rotation of the

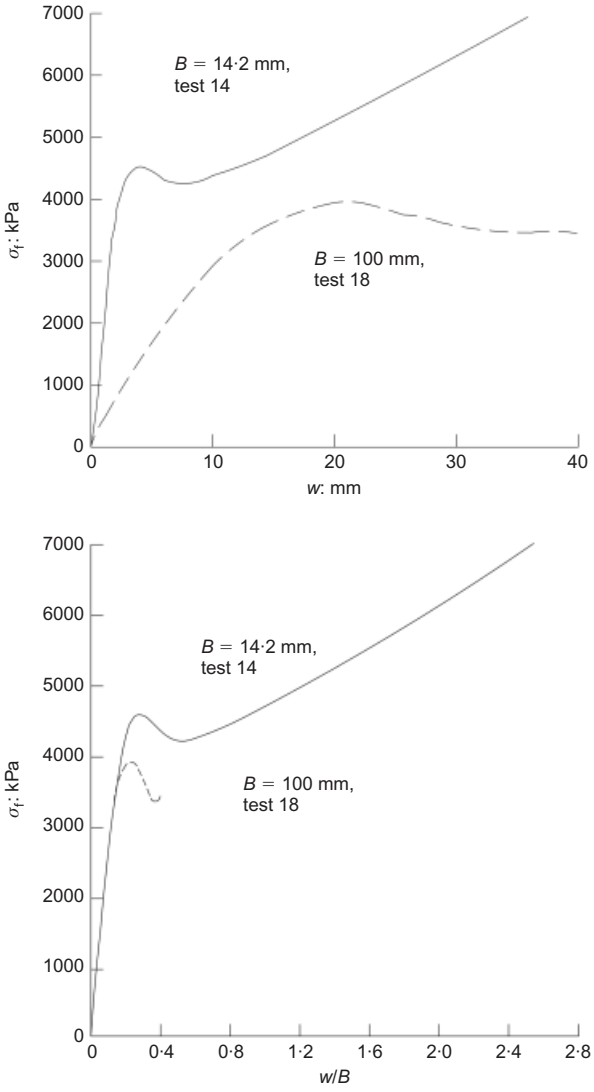

Fig. 9. Comparison between load–settlement response with load–relative settlement response of a footing on sand at 1*g* with $\sigma_o = 10$ kPa

Table 2. Summary of 1*g* test programme

Test no.	Material	e	B: mm	σ_o: kPa	d_{50}: μm	B/d_{50}	Condition
5	Silt	0·63	14·2	100	12	1183	Saturated
6	Silt	0·57	14·2	50	12	1183	Saturated
7	Silt	0·56	14·2	25	12	1183	Saturated
8	Silt	0·57	14·2	10	12	1183	Saturated
9	Silt	0·55	14·2	200	12	1183	Saturated
12	Sand	0·58	14·2	50	600	24	Dry
13	Sand	0·58	14·2	25	600	24	Dry
14	Sand	0·58	14·2	10	600	24	Dry
15	Sand	0·58	14·2	100	600	24	Dry
16	Sand	0·58	14·2	200	600	24	Dry
17	Sand	0·58	100	25	600	167	Dry
18	Sand	0·58	100	10	600	167	Dry
19	Sand	0·59	100	100	600	167	Dry
20	Sand	0·57	100	200	600	167	Dry
21	Sand	0·57	100	50	600	167	Dry
23	Sand	0·58	100	5	600	167	Saturated
24	Sand	0·63	14·2	25	600	24	Saturated
25	Sand	0·64	100	5	600	167	Saturated
26	Sand	0·56	100	5	600	167	Saturated
28	Silt	0·58	14·2	5	12	1183	Saturated

principal stress direction. He proposed an extension of the work of Prandtl (1920) and Reissner (1924) for plane footings with initial burial: see Fig. 10. The soil within region abc of Fig. 10 is conservatively taken to act as a hydrostatic fluid, developing no shear resistance. The surcharge σ_o is therefore taken to act on plane bc sloping at angle β to the horizontal. The rotation of principal stress direction, θ, in the fan is simply $(\pi/2 + \beta)$. The penetration effects of a strip footing on frictional weightless soil can now be incorporated in

$$\sigma_f = \sigma_o k_p e^{2\theta \tan\phi} \tag{1}$$

where $\theta = (\pi/2) + \beta$ and $0 \leqslant \beta \leqslant \pi/2$. When $\beta = 0$, the footing is at the surface and $\theta = \pi/2$

$$\sigma_f = \sigma_o k_p e^{\pi \tan\phi}$$

When $\beta = \pi/2$, the footing is at a critical depth D_c, that is, all additional rotation of principal stress has been exhausted and $\theta = \pi$

$$\sigma_f = \sigma_o k_p e^{2\pi \tan\phi}$$

It is now clear that, for $0 \leqslant D \leqslant D_c$, the penetration effects can be treated as a problem of gradual additional rotation of principal stress. The bearing capacity equation can now be treated as a simple geometry problem that relates penetration D to the additional rotation β.

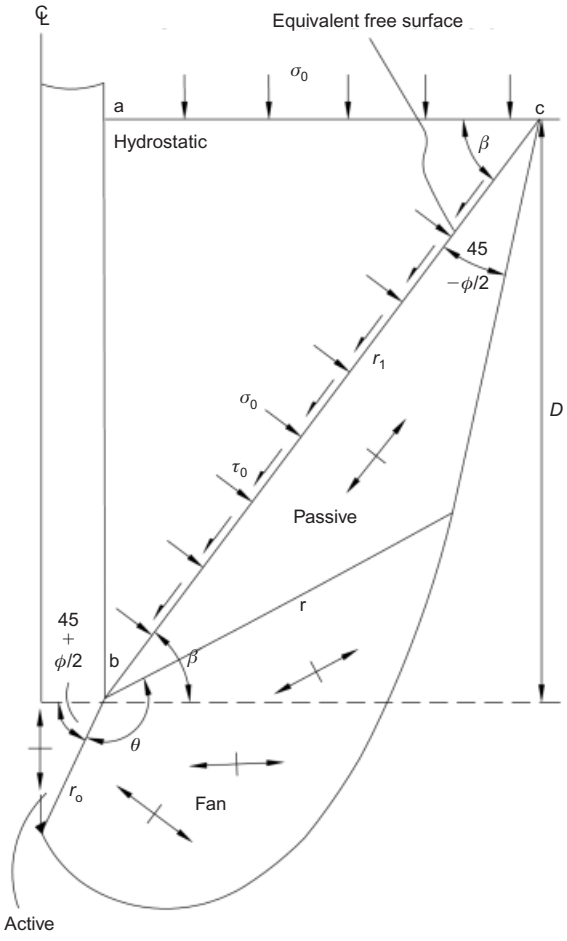

Fig. 10. Extended stress field to account for penetration

It can be shown that

$$D = \frac{B \sin\beta \cos\phi e^{\theta \tan\phi}}{2 \cos(\pi/4 + \phi/2) \sin(\pi/4 - \phi/2)} \tag{2}$$

where $\theta = \pi/2 + \beta$. For $D < D_c$, β can be calculated from equation (2), and when it is substituted in equation (1), σ_f can be found.

For $D \geqslant D_c$, the footing is at or below a critical depth D_c, where $\beta = \pi/2$ and $\theta = \pi$, and any further increase in bearing capacity would be attributed to the additional surcharge of the overburden only.

$$D_c = \frac{B \cos\phi e^{\pi \tan\phi}}{2 \cos(\pi/4 + \phi/2) \sin(\pi/4 - \phi/2)} \tag{3}$$

D_c may properly be taken as the demarcation between shallow and deep foundations. With this new definition, it can be said that the bearing capacity of a shallow foundation should be corrected for geometry effects, whereas for deep foundations the correction for overburden alone is sufficient, provided that the rotation in the shear fan is set at π instead of $\pi/2$.

Meyerhof used Fig. 11 to show a typical 20-fold increase in bearing capacity factor for a footing placed at $D = D_c$ in sand developing $\phi = 45°$. In the current tests the depth D is taken to be equal to the observed settlement w, and for a typical settlement $w = 30$ mm, in test 14 with $B = 14{\cdot}2$ mm, we obtain $D/B = 2{\cdot}1$ giving $\beta = 9°$ and offering an enhancement factor of 1·5.

In order to interpret the data from the tests, the bearing capacity coefficient for a rough circular footing on the surface of soil with a given ϕ value was first calculated using the technique suggested by Cox (1962) and Bolton & Lau (1993). This value was then enhanced by Meyerhof's

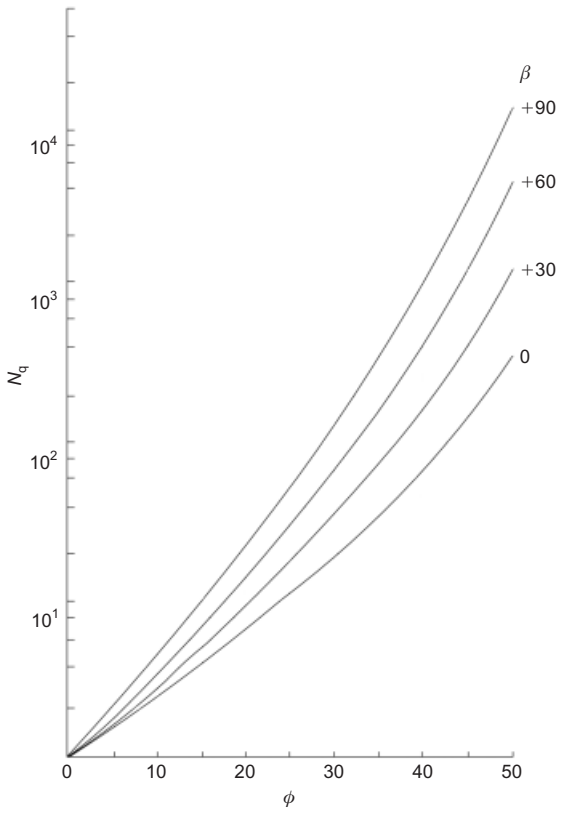

Fig. 11. Effects of shear stress on the equivalent free surface on N_q (after Meyerhof, 1951)

factor, notwithstanding the change from plane strain to axisymmetry. Fig. 12 shows the resulting prediction for N_q against depth ratio D/B.

1g tests: discussion

Figures 13 and 14 compare data with the theory for the 1*g* test of the 14 mm footing on sand and silt respectively. It can be seen that the Meyerhof correction for w/B leads to an interpretation in terms of ϕ remaining approximately constant for $0{\cdot}5 < w/B < 2{\cdot}5$. It may be concluded that the Meyerhof correction is useful in the back-analysis of these axisymmetric footings. Comparing the sand with the silt, it may be seen that the latter mobilised a slightly larger angle

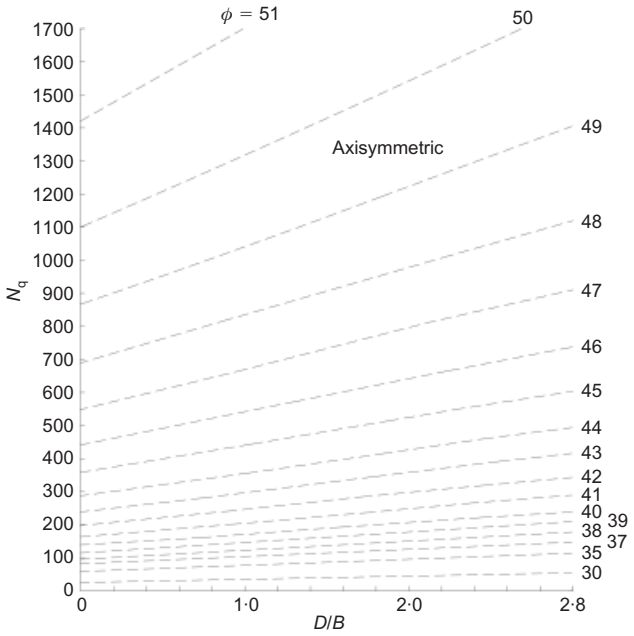

Fig. 12. Theoretical bearing capacity of shallow footing on weightless soil with overburden with shear strength

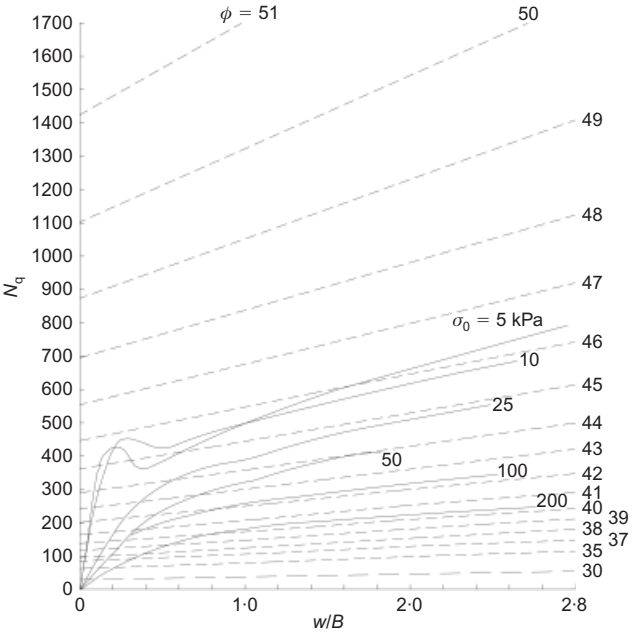

Fig. 13. Interpretation of 1*g* test data by superposing the normalised theoretical and experimental curves for sand, B = 14·2 mm

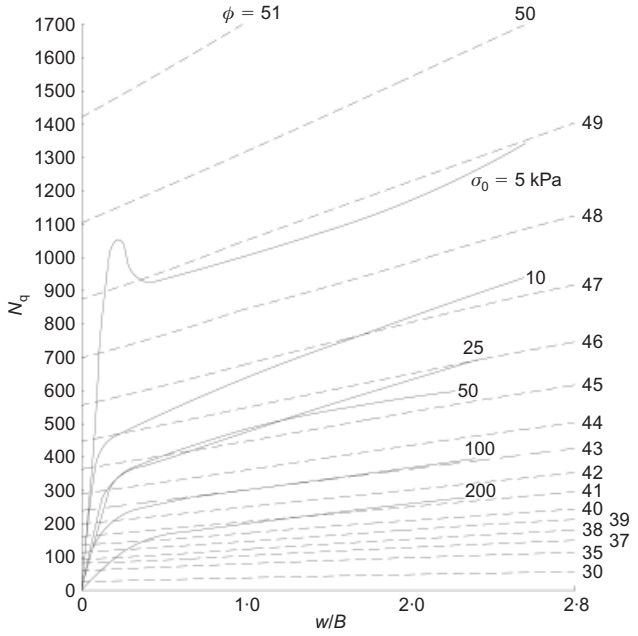

Fig. 14. Interpretation of 1*g* test data by superposing the normalised theoretical and experimental curves for silt, B = 14·2 mm

of shearing: a larger value was expected following the triaxial test results. Fig. 15 shows a similar pattern of penetration for the 100 mm footing on sand: those tests were curtailed at an earlier relative settlement.

Figure 16 shows the use of Meyerhof's w/B correction to obtain the equivalent value of N_q for $w/B = 0$. When a peak ϕ was observed (test m), this was used for the back-extrapolation; otherwise (test n) the asymptotic Meyerhof line was produced back to the N_q axis. Fig. 17 shows the exponential values of N_q versus overburden pressure σ_o, each on a logarithmic scale. A corresponding non-linear scale of ϕ is placed against the $1\log_{10} N_q$ scale. In addition to the data points, the solid lines in Fig. 17 represent the results of the variable-ϕ analyses reported in Fig. 16(a) of the compa-

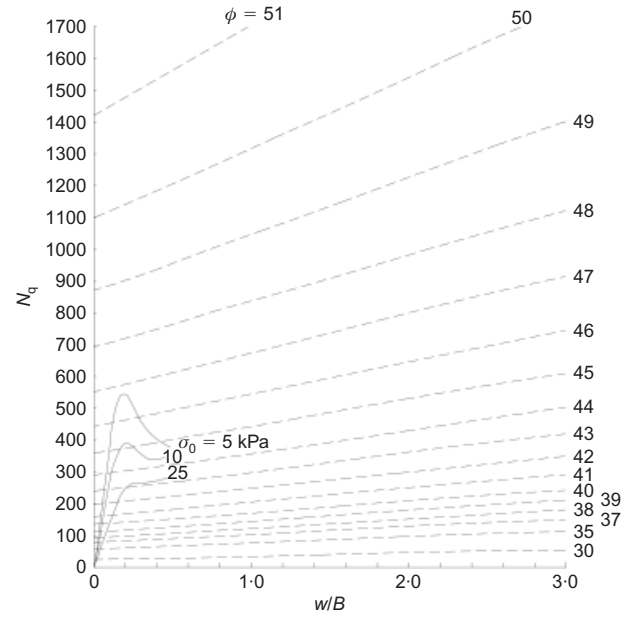

Fig. 15. Interpretation of 1*g* test data by superposing the normalised theoretical and experimental curves for sand, B = 100 mm

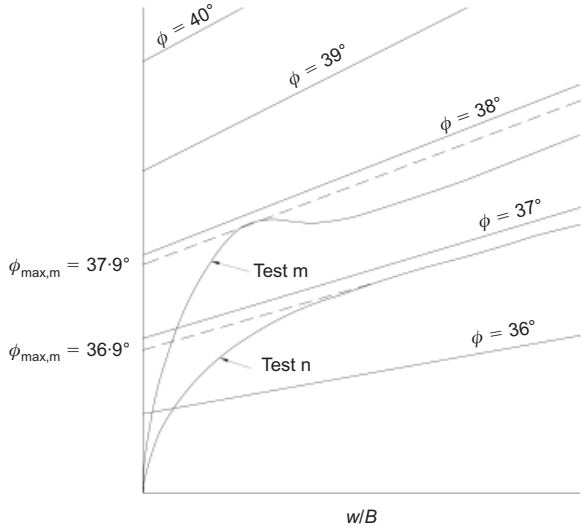

Fig. 16. Schematic diagram showing normalisation of test curves to obtain equivalent N_q for $w/B = 0$

nion paper (Lau & Bolton, 2011), which were based on the best fit to the ϕ–$\log p$ data for the two soils.

The comparison between the variable-ϕ calculation and the 1***g*** test data is within 2° of ϕ, commensurate with the scatter of the triaxial data themselves. The possible scale effects of different footing diameters and different soil particle sizes are seen to be eliminated when triaxial data of ϕ varying with p are used in the calculation of bearing capacity. Footing : particle size ratios between 24 and 1183, and container : footing diameter ratios between 8·5 and 60, apparently create no effect.

CENTRIFUGE MODEL TESTS

The earlier sections have demonstrated how 1***g*** tests, when subjected to a suitable range of surcharge pressures, can yield useful information on the scale effects in tests on footings. The main advantage of the 1***g*** tests is that they can mimic the behaviour of a weightless soil. This advantage, however, becomes its disadvantage when modelling a prototype shallow footing with self-weight. The stresses at homologous points of a scaled-down model should replicate those of a prototype soil construction. This has been shown to be possible if the $1/n$ scale model is subjected to an acceleration field n times that experienced by the prototype in a geotechnical centrifuge.

The same apparatus (Fig. 8) was used for the centrifuge tests, except that the surcharge system was removed and replaced by a frame carrying displacement transducers (Fig. 18). The soil bed was fully submerged in water. The soil model was subjected to an elevated acceleration field of '50***g***' (sand) and '14·2, 50/30 and 100***g***' (silt) in the centrifuge. The whole top surface of the soil model around the punch would be free of surcharge pressure at all times. As before, the average bearing pressure and settlement of the footing were monitored. The details of the tests are recorded in Table 3 (as for the 1***g*** format).

Centrifuge tests: interpretation

For the purposes of interpretation, it was desired to make allowance for the settlement of the footing, as with the 1***g*** tests. In this case, however, the settlement w first produces a

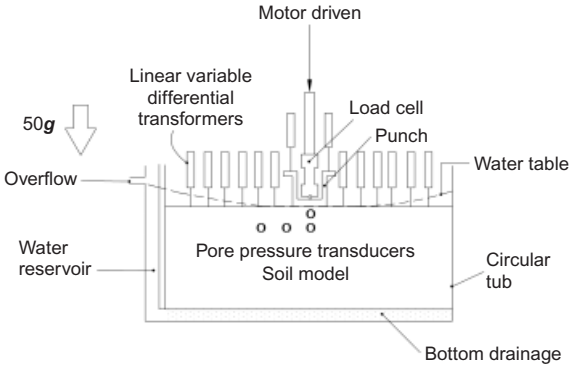

Fig. 18. Model footing apparatus

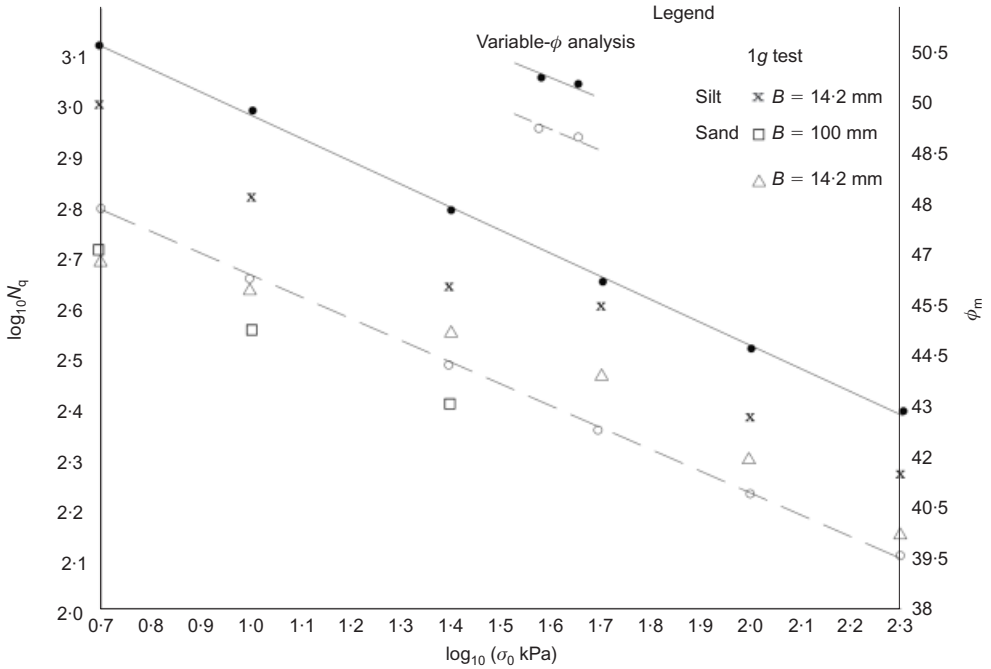

Fig. 17. Calculated and experimental results of the 1*g* tests

Table 3. Summary of centrifuge model tests

Test no.	Material	e	B: mm	n	d_{50}: μm	B/d_{50}	Condition
101	Silt	0·63	100	50***g***/30***g***	12	8333	Saturated
102	Sand	0·61	100	50***g***	600	166·7	Saturated
104	Silt	0·61	14·2	100***g***	12	1183·3	Saturated

significant surcharge effect due to self-weight, enhancing the bearing capacity by a $\gamma' w N_q$ term, and second creates a geometrical enhancement of that term using Meyerhof's construction, as described earlier. These effects create a strong w/B enhancement of the basic bearing capacity of a surface footing for which N_γ was calculated as before on the basis of a rough circular footing on constant-ϕ soil (Bolton & Lau, 1993).

Figures 19 and 20 show data from test 102 for a 5 m (prototype) footing on sand and test 104 for a 1·42 m footing on silt respectively. As before, the w/B correction led to an understanding of the steady increase in bearing pressure with settlement, during plastic penetration. There is no evidence of any softening to $\phi < \phi_{max}$. Back-figuring to $w/B = 0$ permitted the estimation of N_γ in each case. A similar extrapolation procedure was used in test 101, but the interpretation was less secure, because the centrifuge acceleration had to be reduced halfway through the test in order for the loading system to be capable of creating a bearing failure.

Centrifuge tests: discussion

The centrifuge data, back-analysed for N_γ in the way described, are plotted against $\log_{10}B$ (metres prototype) in Fig. 21. Here they are compared with the best-fit lines drawn over the variable-ϕ analyses described in the companion paper (Lau & Bolton, 2011) and plotted in Fig. 17(a) of that paper. It will be seen that the error is within $\pm 1°$, which is as small as it could be, considering the scatter in the original triaxial test data. It can therefore be concluded that there is no discernible relative particle size effects for B/d_{50} varying from 165 to 8333. This observation is consistent with the recommendation by Kusakabe (1995). There are also no measurable chamber effects when $\phi_{tub}/B \geqslant 8{\cdot}5$ and $H_{tub}/B \geqslant 3{\cdot}5$, which is in general agreement with the results reported by Bagge & Christensen (1977).

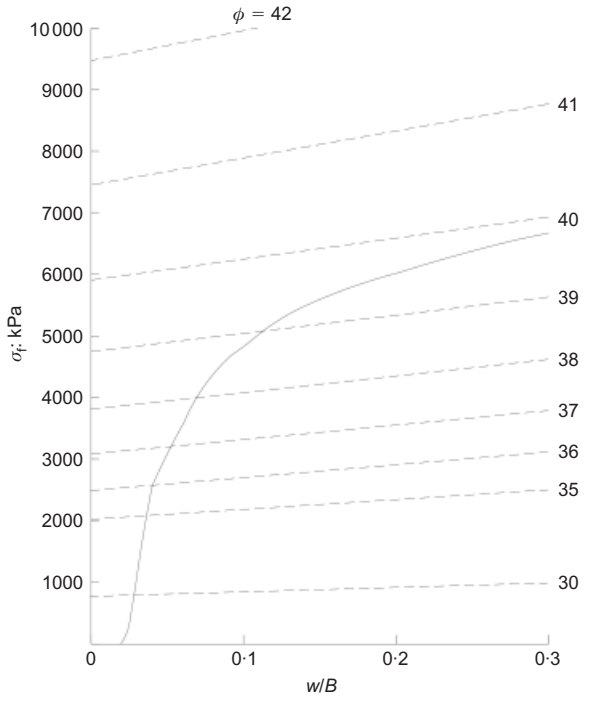

Fig. 19. Interpretation of centrifuge test data by superposing the theoretical and experimental curves for sand, $B = 100$ mm at 50*g*, test 102

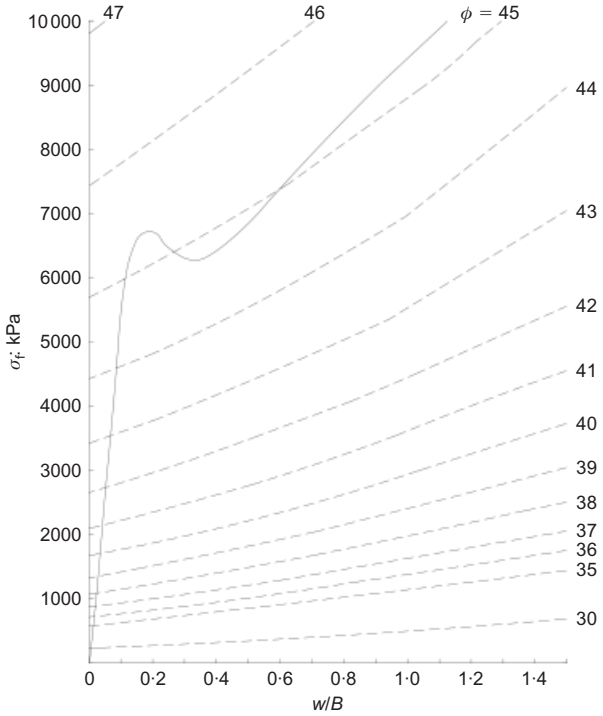

Fig. 20. Interpretation of centrifuge test data by superposing the theoretical and experimental curves for silt, $B = 14{\cdot}2$ mm at 100*g*, test 104

CONCLUSIONS

Tests on small footings bearing on a sand and a silt with similar, but not identical, mechanical properties have been carried out both at 1***g*** under surcharge, and in a centrifuge. Interpretation of the test data demanded that a correction be made for settlement effects, and this was achieved using established techniques. The axisymmetric bearing capacity coefficients were calculated for zero penetration but constant-ϕ following Cox (1962), and Meyerhof's construction (Meyerhof, 1951) was used to correct for geometry effects. This led to an empirical demonstration that bearing capacity coefficients reduce approximately linearly with stress level, on a $\log_{10}$-$\log_{10}$ plot.

Independent analytical estimates of bearing capacity were made based only on the variation of ϕ with mean stress p in triaxial tests, and using the method of characteristics. The comparison between measurements and calculations was

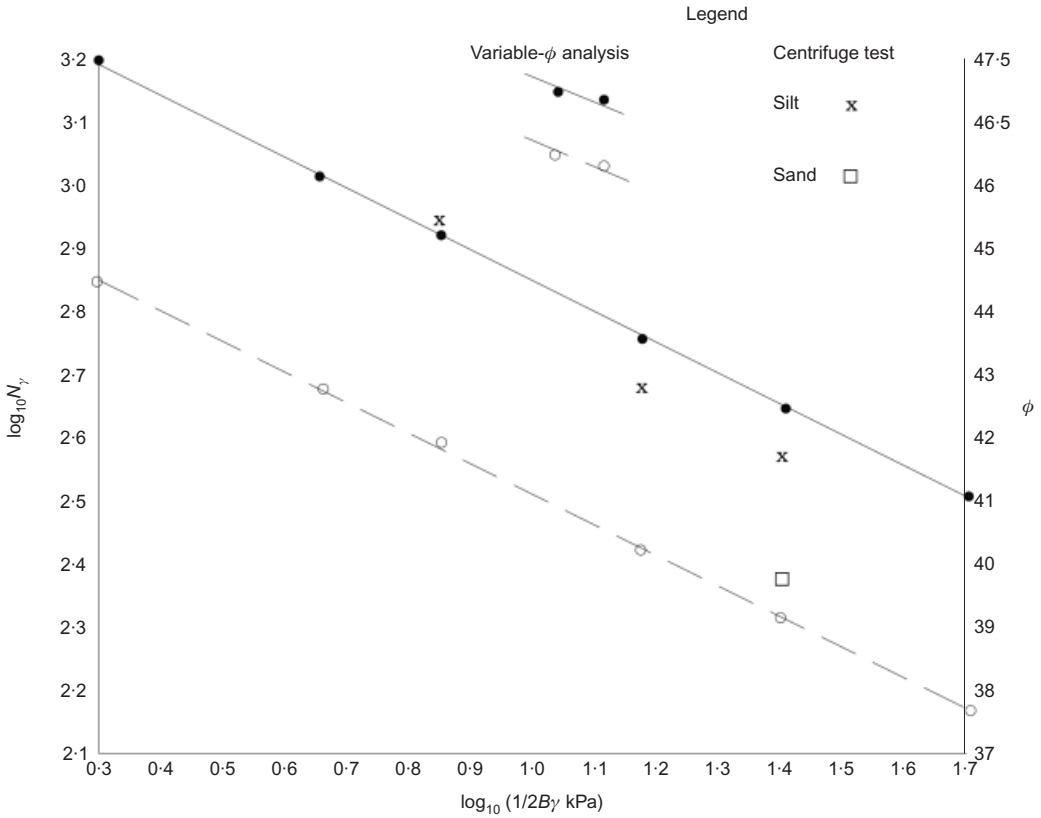

Fig. 21. Calculated and experimental results of the centrifuge tests

excellent, lying within $\pm 2°$ scatter observed in the triaxial test results themselves.

There is no strong evidence that anisotropy (strength reduction for shearing parallel to bedding planes) should have been taken into account. Tatsuoka *et al.* (1991) reported up to 15% loss of ϕ on plane shearing of bedding planes created after pluviation of dense sand samples. However, they also reported that this minimum plane-strain strength was similar to that measured in conventional triaxial compression tests with horizontal bedding. Apparently, the use of ϕ from triaxial compression tests has been adequate in the present back-analysis of circular footings.

Similarly, there is no strong evidence that progressive failure has taken place: peak ϕ values offer reasonable correlations with the peak loads observed in the model tests. Shear bands have previously been observed to propagate progressively downwards from the edge of strip footings on sand. Kimura *et al.* (1985) associated 'scale effects' with these progressive distortions, while not accounting for the effects of ϕ decreasing under increased confining stress. After some 1***g*** and centrifuge tests, the sand models that had horizontal colour marker beds were set by sugar syrup and sectioned for visual inspection. Likewise, the silt model inserted with vertical lead threads was X-rayed (Lau, 1988). No such shear band propagation was observed in the current tests on circular footings, but more tests should be carried out to confirm this observation.

A wide range of footing : container and footing : particle size ratios was investigated, and no geometrical scale effect could be discerned. This suggests that the reduction in ϕ with increase in confining stress is the only significant 'size effect' determining the vertical bearing capacity of the model footings on sand and silt used in these experiments.

The VARIPHI program was used for the calculation of bearing capacity based on ϕ varying with p, as described in the companion paper (Lau & Bolton, 2011). This also demonstrated that an almost identical solution could be generated using constant-ϕ analyses, and therefore using existing bearing capacity factors, if the appropriate value of ϕ_m is used. It was shown that, for surcharge effects only, $P_m = 2\sqrt{\sigma_f \sigma_o}$, whereas for self-weight effects only, $P_m = 13\sqrt{\sigma_f 0{\cdot}5B\gamma'}$. These semi-empirical rules could replace Meyerhof's suggestion of $P_m = \sigma_f/10$ for circular footings.

ACKNOWLEDGEMENTS

The first author is grateful for the financial support provided by the Hong Kong Croucher Foundation. The authors would like to thank the technical staff of the Cambridge University Soil Mechanics Group for their assistance.

NOTATION

All stresses are effective stresses unless otherwise stated.

B	width or diameter of footing
B/d_{50}	footing size/particle size ratio
c	cohesion
D	initial embedment of footing
D_c	critical depth of footing
d_{50}	mean particle size
e	voids ratio
e_{min}	minimum voids ratio
$\boldsymbol{g}$	acceleration due to Earth's gravity
H_{tub}	height of tub
I_D	relative density
k_p	coefficient of passive earth pressure
N_c	bearing capacity factor (cohesion) ($= \sigma_f/c$)
N_q	bearing capacity factor (surcharge) ($= \sigma_f/\sigma_o$)
N_γ	bearing capacity factor (self-weight) ($= \sigma_f/0{\cdot}5B\gamma$)
p	mean stress ($= (\sigma_1 + \sigma_2 + \sigma_3)/3 \approx (\sigma_1 + \sigma_3)/2$)
P_m	equivalent mean working stress

r radius
s mean stress ($= (\sigma_1 + \sigma_3)/2$)
w settlement
w/B relative settlement
β equivalent relative settlement angle
γ bulk density of soil
θ principal stress rotation
σ_f bearing capacity
σ_r cell pressure
σ_o surcharge
ε_a axial strain
ε_v volumetric strain
τ_o shear stress acting on the free equivalent surface
ϕ secant angle of friction
ϕ_{crit} critical state angle
ϕ_{max} maximum angle of friction
ϕ_{mob} mobilised angle of friction
ϕ_{tub} diameter of tub

REFERENCES

Bagge, G. & Christensen, S. N. (1977). Centrifuge testing on the bearing capacity of circular footings on the surface of sand. In *Dialog 77, 20th anniversary*, pp. 337–346. Lyngby: Denmarks Ingeniorakademi, Bygningsafdelingen.

Bolton, M. D. (1986). The strength and dilatancy of sands. *Géotechnique* **36**, No. 1, 65–78, **doi**: 10.1680/geot.1986.36.1.65.

Bolton, M. D. & Lau, C. K. (1993). Vertical bearing capacity factors for circular and strip footings on Mohr–Coulomb soil. *Can. Geotech. J.* **30**, No. 6, 1024–1033.

Cerato, A. B. & Lutenegger, A. J. (2007). Scale effects of shallow foundation bearing capacity on granular material. *J. Geotech. Geoenviron. Engng* **133**, No. 10, 1192–1202.

Corte, I. F. (1989). General report, model testing: geotechnical model tests. *Proc. 12th Int. Conf. Soil Mech. Found. Engng, Rio de Janeiro* **4**, 2553–2571.

Cox, A. D. (1962). Axially-symmetric plastic deformation in soils. II: Indentation of ponderable soils. *Int. J. Mech. Sci*. **4**, No. 5, 371–380.

De Beer, E. E. (1965a). The scale effects on the phenomenon of progressive rupture in cohesionless soils. *Proc. 6th Int. Conf. Soil Mech. Found. Engng, Montreal* **2**, 13–17.

De Beer, E.E. (1965b). Influence of the mean normal stress on the shearing strength of sand. *Proc. 6th Int. Conf. Soil Mech. Found. Engng, Montreal* **1**, 165–169.

Griffith, A. A. (1921). The phenomena of rupture and flow in solids. *Phil. Trans. R. Soc. London Ser. A*, **221**, No. 582–593, 163–197.

Kimura, T., Kusakabe, O. & Saitoh, K. (1985). Geotechnical model tests of bearing capacity problems in a centrifuge. *Géotechnique* **35**, No. 1, 33–45, **doi**: 10.1680/geot.1985.35.1.33.

Kusakabe, O. (1995). Foundations. In *Geotechnical centrifuge technology* (ed. R. N. Taylor), pp. 118–167. London: Blackie Academic & Professional.

Lau, C. K. (1988). *Scale effects in tests on footings*. PhD thesis, University of Cambridge.

Lau, C. K. & Bolton, M. D. (2011). The bearing capacity of footings on granular soils. I: Numerical analysis. *Géotechnique*, **doi**: 10.1680/geot.7.00206.

LeBlanc, L. (1981). Tracing the causes of rig mishaps. *Offshore*, March, 51–62.

Meyerhof, G. G. (1951). The ultimate bearing capacity of foundations. *Géotechnique* **2**, No. 4, 301–332, **doi**: 10.1680/geot.1951.2.4.301.

Muhs, H. (1965). Discussion: On the phenomenon of progressive rupture in connection with the failure behaviour of footings in sand. *Proc. 6th Int. Conf. Soil Mech. Found. Engng, Montreal* **3**, 419–421.

Ovesen, N. K. (1975). Centrifuge testing applied to bearing capacity problems of footings on sand. *Géotechnique* **25**, No. 2, 394–401, **doi**: 10.1680/geot.1975.25.2.394.

Ovesen, N. K. (1979). Panel discussion: The scaling law relationship. *Proc. 7th Eur. Conf. Soil Mech. and Found. Engng, Brighton* **4**, 319–323.

Prandtl, L. (1920). Über die harte plastischer korper (On the hardness of plastic bodies). *Nachr. kgl. Ges. Wiss. Gottingen (Math.-phys. Klasse)*, 74–85.

Randolph, M., Cassidy, M., Gourvenec, S. & Erbrich, C. (2005). Challenges of offshore geotechnical engineering. *Proc. 16th Int. Conf. Soil Mech. Geotech. Engng, Osaka* **1**, 123–176.

Reissner, H. (1924). Zum Erddruckproblem. In *Proc. 1st Int. Conf. Applied Mechanics, Delft*, 295–311.

Schofield, A. N. (1980). Cambridge geotechnical centrifuge operations. *Géotechnique* **30**, No. 3, 227–268, **doi**: 10.1680/geot.1980.30.3.227.

Tatsuoka, F., Okahara, M., Tanaka, T., Tani, K., Morimoto, T. & Siddiquee, M. S. A. (1991). Progressive failure and particle size effect in bearing capacity of footing on sand. *Proceedings of the geotechnical engineering congress*, Boulder, CO, ASCE Special Publ. No. 27, pp. 788–802.

Terzaghi, K. & Peck, R.B. (1948). *Soil mechanics in engineering practice*. New York: John Wiley.

Vesic, A. S. (1963). Bearing capacity of deep foundations in sand. *Highway Research Record*, No. 39, 112–153.

Yamaguchi, H., Kimura, T. & Fuji-i, N. (1976). On the influence of progressive failure on the bearing capacity of shallow foundations in dense sand. *Soils Found*. **16**, No. 4, 11–22.

Yamaguchi, H., Kimura, T. & Fuji-i, N. (1977). On the scale effect of footings in dense sand. *Proc. 9th Int. Conf. Soil Mech. Found. Engng, Tokyo* **1**, 759–798.